FAILURE PRESSURE PREDICTION OF PIPELINES STEEL IN THE PRESENCE OF CORROSION DEFECTS AND PRE-STRAIN

PRAKASH RAJ A/L SUBRAMANIAM

Report submitted in fulfilment of the requirements
for the award of the degree of
Bachelor of Mechanical Engineer

Faculty of Mechanical Engineering
UNIVERSITI MALAYSIA PAHANG

JUNE 2013

ABSTRACT

This projects explains the methods used in predicting the failure pressure of defective pipelines. The failure pressure of defective was estimated for the pipe with the different types of defects. APIX42 steel is chosen for this studies and it must undergoes few machining steps to design a tensile test specimen according to ASTM E8-08M-11. Data obtained from tension test (engineering stress strain) must convert into true stress strain in order to transfer it during simulation (field). Power law is the formula used to convert engineering stress strain to true stress strain. Ultimate strength of APIX42 is predicted at 612 MPa. For modelling part, one quarter of pipeline geometry need to design in MSCPatran software. This study is only focussed on single type of defect. Meshing (element) steps continues after one quarter of geometry is designed. Modelling and simulation is repeated for the different depth (25%, 50% and 75%) of defects and increment in pre-strain. Result obtained after the simulation process must be interpolated to get more accurate failure pressure. Predicted failure pressure is higher for pipeline without presence of pre-strain. Pipeline with the presence of pre-strain, predicted failure pressure is reducing as the amount of pre-strain applied is increases. Three industry models are compared with the finite element result (FEA) for validation. For the lower depth, FEA failure prediction is the highest followed by DNV-RP-F101. ASME B31G and Modified B31G predicted almost same failure pressure but less than FEA and DNV-RP-F101. When the depth increases, DVN-RP-F101 predicted higher value of burst pressure compared to FEA. Whereas Modified B31G and ASME B31G predicted lower failure pressure but getting closer to FEA and DVN-RP-F101. The same phenomena happened when various amount of pre-strain (1kN, 3kN and 5kN) applied, but predicted failure pressure is lower than without pre-strain. By referring to the result, presence of pre-strain is really effected value of failure pressure. Increase in pre-strain will cause losing balance strength in pipelines and leads failure in short time compare to pipelines without pre-strain.

ABSTRAK

Projek ini menjelaskan kaedah kaedah untuk menentukan tekanan kegagalan bagi paip yang mengalami kerosakkan. Tekanan paip rosak perlu ditentukan untuk kerosakkan yang pelbagai. APIX42 adalah jenis paip yang telah dipilih untuk kajian ini dan paip ini perlu menjalani beberapa langkah reka bentuk yang dirujuk daripada ASTM-E8-08M-11. Komposisi kimia dalam APIX42 boleh dikenal pasti melalui ujian spectrometer. Data (Engineering) yang diperolehi daripada ujian ketegangan perlu diolah kepada data yang lebih tepat (true). Keupayaan maksimun APIX42 adalah diangggarkan pada 612 MPa. Untuk pembinaan asas, satu per empat daripada geometri paip perlu dibina dalam Patran. Kajian ini hanya menyentuh kepada satu bahagian kerosakkan. Dimensi untuk paip dan dimensi bagi bahagian yang rosak dirujuk daripada L.U.Xu (2009). Selepas pembinaan asas, perlu diikuti dengan proses menyirat. Untuk analisis yang lebih tepat, tentukan number sirat yang lebih banyak pada kawasan kerosakkan. Anggaran yang diperoleh daripada analisis perlu disisipkan untuk dapatkan nilai yang lebih tepat. Tekanan sebelum dan selepas daripada 612 MPa perlu dicatatkan mengikut masa. Masa kepunyaan kepada 612 MPa perlu disisipkan dan masa tersebut perlu didarabkan dengan tekanan yang dikenakan pada paip. Hasil darab dikenali sebagai tekanan paip pecah. Cara untuk mendapatkan tekanan letus dikenali sebagai von Mises. Tekanan paip pecah juga dipengaruhi oleh tegangan yang bertindak keatas paip. Nilai tekanan sebanyak1 kN, 3 kN dan 5 kN telah diuji untuk dapatkan perbezaan antara satu sama lain. Keputusan menunjukan bahawa tekanan letus menurun apabila nilai ketegangan bertambah. Keputusan telah berbanding dengan kod reka bentuk tersedia untuk paip rosak seperti ASME B31G, Modified B31G dan DNV-RP-F101. Perbandingan dengan kod reka bentuk menunjukkan bahawa tekanan letus FEA memberikan nilai yang lebih tinggi berbanding dengan kod. Daripada keputusan, ASME B31G memberikan nilai yang terendah daripada kod lain.

TABLE OF CONTENT

LIST OF FIGURES

LIST OF TABLE

LIST OF SYMBOLS

P	Load applied
ΔU	Internal strain energy
W	Mechanical work
$\Delta\delta$	Displacement
ε_f	Fracture strain

LIST OF ABBREVIATIONS

ASME	American society mechanical engineering
ASTM	American society for testing and material
API	American Petroleum Institute
FEA	Finite element analysis
PPM	Parts per million
RPM	Revolution per second
SCC	Stress corrosion factor
SIF	Stress intensity factor
SMTS	Specified minimum tensile strength
SMYS	Specified minimum yield strength
SS	Stainless steel
TF	Triaxiality factor

CHAPTER 1

INTRODUCTION

1.1 GENERAL INTRODUCTION

One of the major energy sources that contribute to most of the companies is crude oil. Petroleum or crude oil is a naturally occurring liquid found in formations in the earth consisting of a complex mixture of hydrocarbons (mostly alkenes) of various lengths. Demand for petroleum is increasing year by year. There is a lot of industries growth nowadays and engineers need to provide an efficient pipeline system to supply petroleum to those industries. Moreover majority of companies plants begin to locate on harsh geometry places for safety precautions. In these conditions, underground piping may encountered with frequent soil movement. That particular piping will lose its original strength due to soil movements. The rest of balance strength is depends on pressure exert by petroleum flow itself and third party defects.

To supply sufficient amount of petroleum, large diameter pipeline and small thickness are required. American Petroleum Institute (API) is a united state largest trade association for oil and natural gas industry. A study of failure pressure (burst pressure) is going to be done by selecting few type of material based on API.

The entire specimen need undergo tensile test to get an engineering stress strain diagram. Data for engineering stress strain is convert in true stress stress which need to entered in Patran software for run simulation. Set all the boundary condition in Patran for finite element analysis. Failure pressures are identified from

finite element analysis by von Mises method and compare them with the presence of pre-strain.

1.2 PROBLEM STATEMENT

Most of the petroleum pipelines facing leakages problem due to defects occurred on pipe itself. Corrosion and cracks are the example of defects on pipes. These types of defects happen during installation time by third party and soil's chemical reaction. Pipelines will lose a part of its strength due to this type of phenomena. When the pipeline encountered with soil movements, it will exerted an amount of pressure additional with pre-strain.

Based on literature, there is no proper equation to calculate the burst pressure. Moreover existing equation were only focused on stress based but strain based was ignored. To overcome this issue, a study has planned to find out burst pressure for defective pipes with presence of pre-strain.

1.3 PROJECT SCOPE

1) Material used APIX42 steel
2) Determination of material properties (Tension Test)
3) Finite element analysis using MSCPatran/Marc
4) Burst pressure prediction for various depths of defects with the presence of pre-strain. Validation with industry codes such as ASME B31G, Modified B31G and DNV-RP-F101

1.4 OBJECTIVE

1) Determine failure pressure for defective pipes
2) Understand effect of pre-strain on failure pressure of defective pipes

CHAPTER 2

LITERATURE REVIEW

2.1 EFFECT OF PRE-STRAIN ON FAILURE PRESSURE AND PLASTIC DEFORMATION OF PIPELINES

Most of the underground piping is operating more to longitudinal direction, no matter of tensile or compressive, would reduce the failure pressure of the defected pipelines. When the soil strength acting on the pipeline, a mechanical work is generated to increase the strain energy of the pipe steel;

$$\Delta W = P\Delta\delta + \int_0^{\Delta\delta} \Delta P \, dx = \Delta U \qquad (2.1)$$

where ΔW is the mechanical work falls on pipeline, ΔU is the internal energy gain, P is the external load, and Δδ is the displacement. During plastic region, half of the mechanical work transferred to different type of internal energy and mechanical work including lattice dislocation displacement different. By doing this, in the plastic region highest pre-strain will be 0.25%. The mechanical work is thus converted into the elastic strain energy. This additional strain energy decreases the demand of internal pressure to result in failure of the pipe, and consequently, the failure pressure decreases with the applied tensile or compressive pre-strain.

For the new type of corrosion defects, plastic deformation area increases with the application of pre-strain. Since number of internal energy absorbed directly proportionally to the size of the plastic deformation, it is seen from that the tensile pre-strain is more effective to result in internal strain than the compressive one. Compressive pre-strain results higher value in failure pressure prediction compared to tensile pre-strain. Furthermore, it is realized that pre-strain would harden the pipe steel kinematically and affect the distribution of failure pressure. Since this work focused on the stress and strain determination at corrosion defects in the presence of pre-strain, a complex distribution of the hardening effect would not be covered (Cheng, 2011).

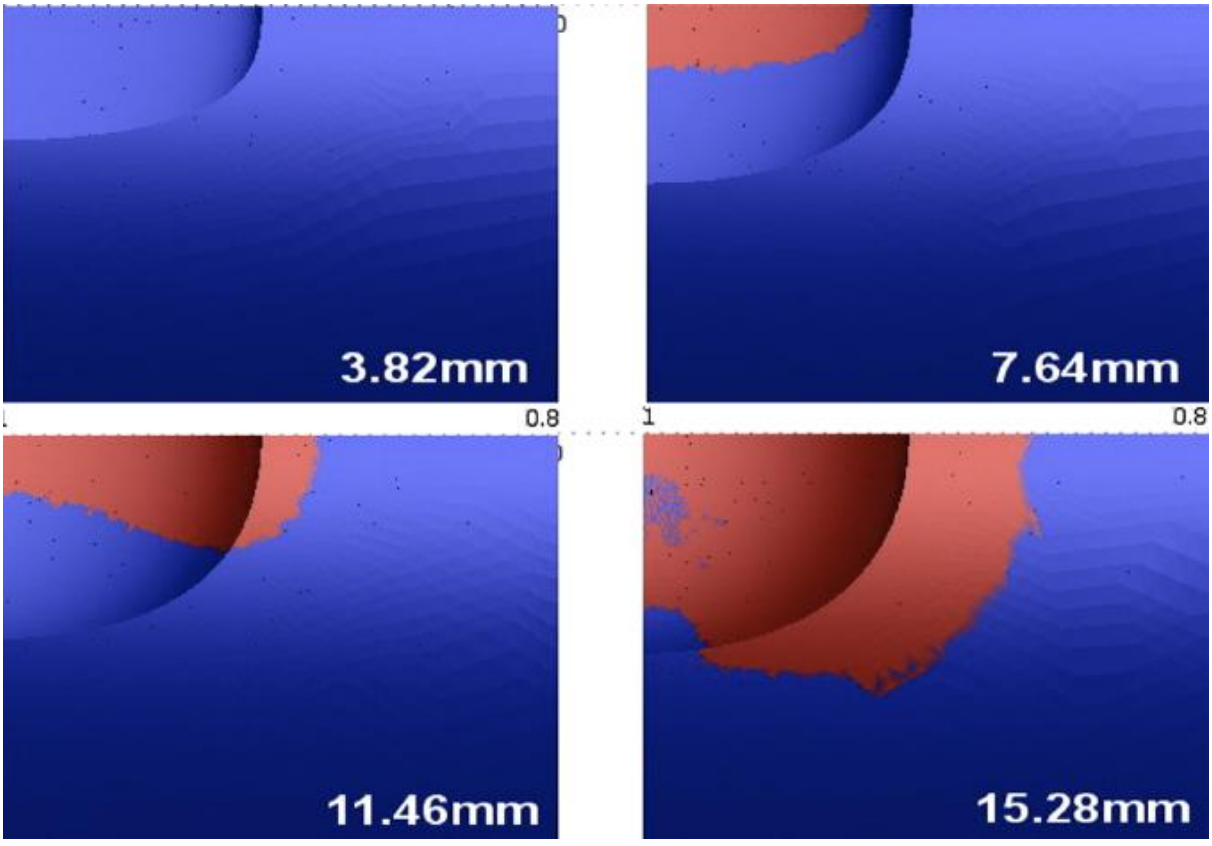

Figure 2.1: Cross-sectional views of the plastic deformation area

Source: Cheng (2011)

2.2 QUALITY EVALUATION OF THE RESISTANCE OF PIPELINES

For both evaluated steel will be the same in the chapter of microcracks. For thin and widely corroded microcracks, frequently can be observed with corrosion micropits around previous inclusions. A big part of microcracks either initiated apparently on inclusions or corrosion pits connected within inclusions were present in their paths.

Research on cracks can be divided into many branches. This can be explained by a more significant local plastic deformation around hard inclusions, especially in the pre-strained specimens. The SCC (stress corrosion cracking) process was probably enhanced step by step by local microstresses which linked with the local plastic deformation and partly by the material interface between inclusions and basic material giving rise to microcells.

Surface microcracks relief is one of the type which considered hazardous from the point of view of a possible subsequent growth by coalescence lines of microcracks. Evethough similar fenomena were found more frequently in the X60 steel, in the CCSN 11375 steel occurred.

An example of one of the most expressive surface lines of microcracks, close to the X60 weld, has been documented the X60 steel, such the lines of microcracks were explained by etching a surface structure. The surface structural interfaces between zones containing preferentially pearlite and zones with ferrite were priority nucleation sites of microcracks. The orientation of the microstructure close to the weld in the X60 steel was inclined to the surface. Therefore, in this case, the non-homogeneous zones were more frequent than in basic material. This can be one of the reasons of the mentioned higher sensitivity of this area of the X60 material to SCC.

A similar connection was found also in the X60 basic material, where structurally different surface areas were present due to a non-parallel direction of structural layers in comparison with the surface plane or due to locally homogeneized areas. Such areas probably gave rise to microcells. A partially different character of

microcracks was found on the surface of the fatigue loaded specimen. Microcracks initiated on inclusions frequently, too. They were, however, evidently more frequent and mostly very thin. It demonstrates different corrosive conditions caused either by braking a surface corrosive microfilm due to repeated elastic deformation or by entirely different surface and subsurface conditions different dislocation structures especially around inclusions.

A fundamental question in the SCC process is whether initiated cracks grow or arrest. Although the observed cracks grew only slightly, it did not mean that the whole process arrested. The summarized microcrack length namely grew. It indicated that during further periods, new microcracks initiated rather than the previous ones grew. If the process continues by this way, it could result in a formation of a main crack by crack coalescence even in these conditions (Cerny, 2002).

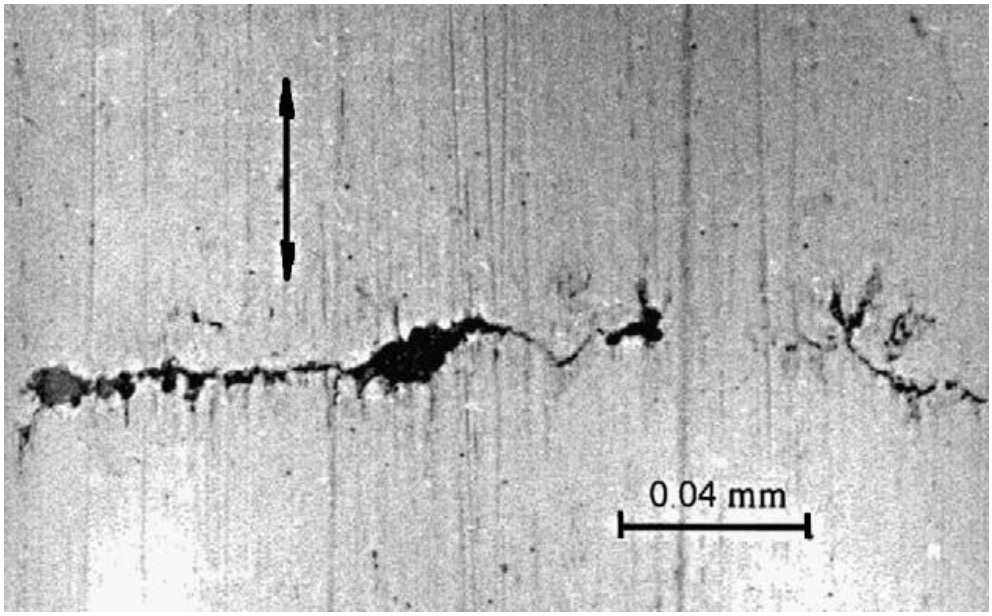

Figure 2.2: Stress corrosion cracking on inclusions in heat affected zone of specimen.

Source: Cerny (2002)

2.3 STRESS CONCERNTRATION CRACK

Brown, powdery scale is covered on the external surface of the pipe. It had rough appearance and contained enumerable number of corrosion pits. Underground pipes is penetrate by cracks which was originated from the pits. Transgranular mode is mainly propagated by cracks, and they were branching in nature. These characteristic are typical of stress corrosion cracking (SCC). Stress corrosion cracks generally undergo extensive branching and proceed in a direction perpendicular to the stresses contributing to their initiation. In general, four conditions are necessary for SCC to occur: (a) susceptible material (b) sustained tensile stress, either residual or applied, (c) aggressive environment containing specific ions, and (d) presence of an electrolyte (water/moisture).

It is known that austenitic stainless steels are susceptible to SCC and hence they need protection for satisfactory working under certain environmental conditions. The SCC in wrought stainless steels is usually transgranular in nature, if the microstructure is not sensitized. In sensitized microstructure, SCC invariably results in intergranular cracking. The microstructural examination confirmed that the pipe was properly heat-treated and there were no microstructural abnormalities. Hence, the SCC in the pipeline was caused due to environmental effects that resulted in transgranular mode of fracture.

Compositional analysis showed that chlorine ion was responsible for the initiation of pitting corrosion on the external surface and subsequent SCC in the pipeline. A chloride concentration of less than 10 ppm is sufficient to cause SCC in austenitic stainless steel if the metal temperature is more than 60 ^{o}C. The operating temperature of the failed pipeline was 72 ^{o}C, which is ideal for chloride induced SCC. The source of chloride was identified to be the insulation material, like glass wool. Chemical analysis revealed that the glass wool contained about 200 ppm of chloride. Chlorides do not cause SCC unless an aqueous phase is present and therefore, it is certain that there was a condensation of water at the hot metal surface.

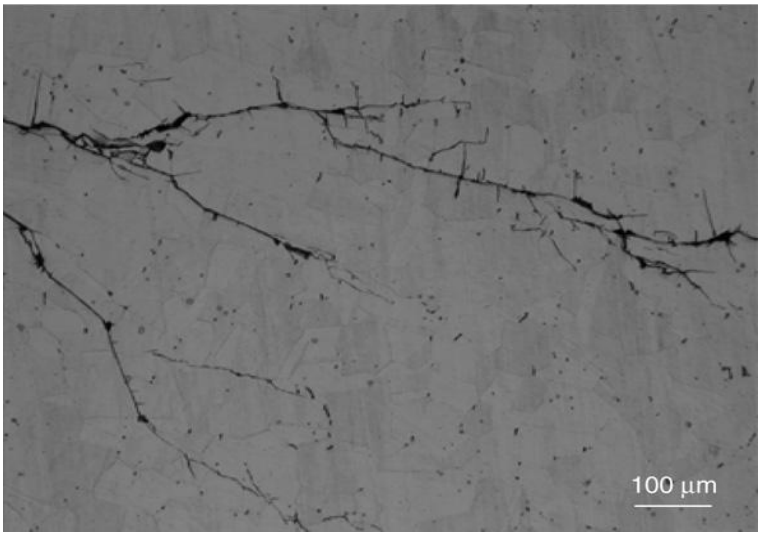

Figure 2.3: Transgranular and intergranular crack propagation

Source: Kumar (2007)

The SS pipeline was wrapped with a protective layer of SS (stainless steel) foil followed by which it was thermally insulated by a layer of glass wool. On removal of the glass wool at the failed region of the pipeline, perforations were observed in the SS foil protective layer. It is, therefore, imperative that SS foil had undergone pitting corrosion first. After this, the protective layer was ineffective and the chlorides from the glass wool could easily migrate to the hot surface of the SS pipeline. As a result, concentrated chlorides had condensed, accumulated in localized regions on the outer surface of the pipeline leading to SCC failure. A concentration of 200 ppm (parts per million) of chlorides in the glass wool at a temperature of about 70 ^{0}C would cause extensive pitting in the SS foil.

Once this protection is destroyed, the pipeline beneath the protective layer is affected. Stainless steel is a bad thermal conductor and hence, there existed a temperature gradient wherein the SS foil was at a lower temperature than that of the outer surface of the pipeline. This facilitated preferential migration of the chlorides to the hot surface of the pipeline and resulted in condensation accumulation of chlorides in localized regions at much higher concentrations (Kumar, 2007).

2.4 FATIGUE OF STRESS CORROSION CRACKS

Cyclic loading of a gas pipeline containing dormant SCC cracks has shown that the SCC cracks extended by fatigue. Although SCC cracks tended to grow at an angle away from the perpendicular in this particular pipeline, the SCC cracks extended by fatigue directly into the material perpendicular to the pipe surface. The expectation was that the SCC cracks would grow rapidly by fatigue in the depth direction and slowly in the axial direction at the beginning of the fatigue crack growth, as modelled. Based on previous fatigue crack growth experiments in X65 pipeline steels and fatigue crack growth modelling, it was expected that the fatigue crack aspect ratio would tend to approach and grow at a constant aspect ratio between 0.31 (experimentally determined value) and 0.38 (computational model based value).

An unexpected result of the analysis of fracture surfaces in this work was that SCC cracks barely grew at all by fatigue along the free surface of the pipe in many cases, especially when there were other cracks nearby. Despite the scatter in results of axial direction growth, all SCC cracks seemed to grow by fatigue unimpeded in the depth wise direction. An SCC crack tended to grow perceptibly along the surface by fatigue only if other cracks were nearby that could positively interact with it and accelerate its crack growth or if it seemed to be isolated from other cracks nearby.

It is not known whether the cracks would approach a certain value if they had been left to grow indefinitely and the pipe thickness was large enough to allow such growth. The crack aspect ratios measured in this work suggest that it possible for SCC cracks to extend by fatigue so as to achieve a crack aspect ratio between 0.31 and 0.38 as previously reported.

SCC crack aspect ratio does not seem to be an indicator of how much the crack will grow by fatigue. This wide scatter in aspect ratio results seems to suggest that crack interaction can have a large influence on the crack propagation by fatigue of SCC cracks.

Due to the nature of SCC crack colonies, it is common to find many SCC cracks in close proximity to each other. This closeness between cracks adds to the complexity of SCC and fatigue crack growth due to the possible crack interaction that occurs between nearby cracks. Based on the results presented here, it can be seen that crack interaction can be a very complex matter, depending on the SIF (stress intensity factor) at each point along the crack front. Parkins' guideline of $0.025 + 0.14 \times 2c$ would imply that the interacting distance for the cracks examined would be up to 4 mm. By this definition, most of the examined cracks were classified as 'interacting' with at least one neighbouring crack, as the crack density within the SCC colony was considerable.

Even though all of the examined cracks could be deemed to be influenced by neighbouring cracks to an extent, some trends have been observed. The deeper the original SCC crack, the deeper the fatigue crack will tend to grow. If two collinear cracks grow at a similar angle they can positively interact and grow towards each other and coalesce, but if they grow at different (or even opposing) angles they seem to negatively interact, and tend not to grow towards each other at all.

SCC cracks that are in the process of coalescing by SCC tend to show a high fatigue crack growth rate in the coalescing region, indicating that the SIF would have been higher at that point (due to crack interaction) than at the surface tips away from the coalescing region (hence faster crack growth rate towards the material than along the surface). Based on previous modelling, in these cases it would be expected that the coalescing cracks would continue to grow in the depth direction until the new fatigue crack front is a single semi-ellipse.

After that shape is achieved, the crack would then resume growing along the surface. If two non collinear cracks grow away from each other, there seems to be no interaction at all between the two cracks. If two non collinear cracks grow towards each other they can coalesce and change crack direction close to the perpendicular (as if they tend to neutralise each other's inclined crack propagation angle). Once these cracks have coalesced below the surface and are subject to a cyclic load, these cracks can develop fatigue cracks that extend from the coalescence point upwards towards the free

surface (showing up as hoop oriented cracks joining SCC cracks), as well as the main crack tip propagating further into the material by fatigue. This complex scenario has been shown to be able to cause one such crack interaction and growth to result in a through wall crack as illustrated in (Gamboa, 2007).

2.5 EFFECT OF NOTCH MATERIAL PROPERTY GRADIENT ON LIFE PREDICTION WITH LOCAL APPROACH

For fatigue evaluation of notched specimen, three approaches were usually used: nominal stress method, local stress strain method and energy method. Usually, material property gradient was not under consideration when local method was utilized. However, the above analysis indicated that the maximum stress and maximum strain do not always fall on the same point when there is material property gradient at notch root. Hence, which point should be selected for life prediction would remain a problem. One damage equation used frequently is the Morrow modified Manson-Coffin damage equation.

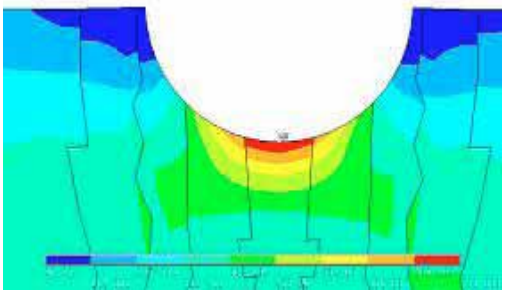

Figure 2.4: von Mises stress distribution

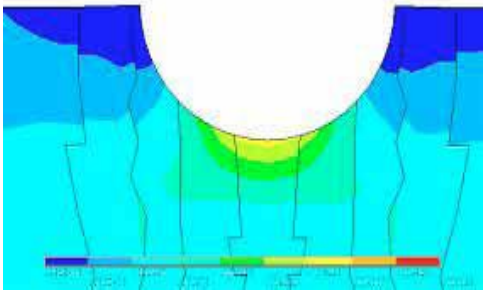

Figure2.5: von Mises strain distribution

Source: Wang (2011)

As for the fatigue strength coefficient, Eleiche's study had showed which increase with material hardness. Thus for life prediction, if stress strain on several different nodes is selected, the node with the shortest life predicted may not always fall on the same node. If the shortest predicted life of the several nodes can be treated as fatigue life prediction results, as well as fatigue crack initiation site, then conclusion can be drawn that for notched specimen with material gradient at notch root, the node with the maximum stress value may be not where the maximum strain locates. Above